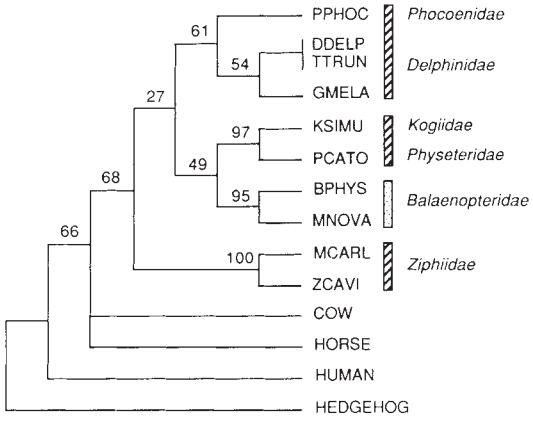

FIG. 2 Bootstrap consensus tree based on published myoglobin sequences. The majority rule bootstrap consensus tree favours the grouping of the Ziphiidae with the sperm whale–baleen whale clade at a bootstrap value of 36%. Numbers represent bootstrap values (100 replications). Analysis was done with PAUP[17] using a stepmatrix (PROTPARS) which gives the minimum number of amino-acid replacement substitutions needed to convert one amino acid to another. Abbreviations of the species names are as in Fig. 1, except MCARL, *Mesoplodon carlhubbsi* (Hubbs' beaked whale); ZCAVI, *Ziphius cavirostris* (Goose-beaked whale). Species were chosen to be as close as possible to the ones used for our mitochondrial sequence analysis. The inclusion of other cetacean species for which myoglobin sequences are available (*Balaenoptera acutorostrata, B. borealis, Eschrichtius gibbosus, Inia geoffrensis, Phocoena dalli, Stenella attenuata, Orcinus orca*) and further outgroups (sheep and red deer) did not change the topology but tended to lower the bootstrap values.

but hinted that toothed whales might not be monophyletic. We anticipate that more molecular data will be collected that will test the phylogeny of cetaceans. □

Received 7 August; accepted 16 November 1992.

1. Flower, W. H. *Proc. zool. Soc. Lond.* **1883,** 466–513 (1883).
2. Van Valen, L. *Bull. Am. Mus. nat. Hist.* **132,** 1–126 (1966).
3. Szalay, F. S. *Am. Mus. nat. Hist. Nov.* **2361,** 1–26 (1969).
4. Gingerich, P. D., Wells, N. A., Russell, D. E. & Shah, S. M. I. *Science* **220,** 403–406 (1983).
5. Gingerich, P. D. Smith, B. H. & Simons, E. L. *Science* **249,** 154–157 (1990).
6. Goodman, M., Czelusniak, J. & Beeber, J. E. *Cladistics* **1,** 171–185 (1985).
7. Irwin, D. M., Kocher, T. D. & Wilson, A. C. *J. molec. Evol.* **32,** 128–144 (1991).
8. Milinkovitch, M. C. *J. evol. Biol.* **5,** 149–160 (1992).
9. Barnes, L. G., Doming, D. P. & Ray, C. E. *Mar. Mammal Sci.* **1,** 15–53 (1985).
10. Barnes, L. G. & Mitchell, E. in *Evolution of African Mammals.* (ed. Maglio, V. J. & Cooke, H. B. S.) 582–602 (Harvard University Press, London, 1978).
11. Mindell, D. P. & Honeycutt, R. L. *A. Rev. Ecol. Syst.* **21,** 541–566 (1990).
12. Allard, M. W. *et al. Proc. natn. Acad. Sci. U.S.A.* **89,** 3972–3976 (1992).
13. Miyamoto, M. M., Kraus, F. & Ryder, O. A. *Proc. natn. Acad. Sci. U.S.A.* **87,** 6127–6131 (1990).
14. Gatsey, J., Yelon, D., DeSalle, R. & Vrba, E. S. *Molec. Biol. Evol.* **9,** 433–446 (1992).
15. Anderson, S. *et al. J. molec. Biol.* **156,** 683–717 (1982).
16. Eperon, I. C. *et al. Nature* **286,** 460–467 (1980).
17. Swofford, D. L. *Phylogenetic Analysis Using Parsimony* Version 3.0s (Illinois Natural History Survey, Champaign, 1991).
18. Saitou, N. & Nei, M. *Molec. Biol. Evol.* **4,** 406–425 (1987).
19. Felsenstein, J. *PHYLIP* Version 3.4.1. (University of Washington, Seattle, 1991).
20. Felsenstein, J. *Evolution* **39,** 783–791 (1985).
21. Novacek, M. J. *Nature* **356,** 121–125 (1992).
22. Schlötterer, C., Amos, B. & Tautz, D. *Nature* **354,** 63–65 (1991).
23. Kraus, F. & Miyamoto, M. M. *Syst. Zool.* **40,** 117–130 (1991).
24. Arnason, U., Gullberg, A. & Widegren, B. *J. molec. Evol.* **33,** 556–568 (1991).
25. Czelusniak, J. *et al.* in *Current Mammalogy* Vol. 2 (ed. Genoways, H. H.) 545–572 (Plenum, New York, 1990).
26. Higgins, D. G. & Sharp, P. M. *Gene* **73,** 237–244 (1988).
27. Gutell, R. R. & Fox, G. E. *Prog. Nucleic Acid Res.* **16** (suppl.), R175–R313 (1988).
28. Gutell, R. R., Weiser, B., Woese, C. & Noller, H. F. *Nucleic Acids Res.* **32,** 155–215 (1985).
29. Kocher, T. D. *et al. Proc. natn. Acad. Sci. U.S.A.* **86,** 6196–6200 (1989).
30. Meyer, A., Kocher, T. D., Basasibwaki, P. & Wilson, A. C. *Nature* **347,** 550–553 (1990).
31. Palumbi, S. R. *The Simple Fool's Guide to PCR* (Department of Zoology, University of Hawaii, Honolulu, 1991).

ACKNOWLEDGEMENTS. We thank F. Coignoul, M. Demeurichy, J. L. Don, J. Oporto, J. Reyes, S. Sadove, J. Smolders, L. Tolpe, P. Vrana and K. Van Waerenbeek for samples; J. Bouillon, J. Dumont, J. Pasteels, J. Powell, G. Vassart and G. Wagner for financial and technical assistance; V. Milinkovitch for drawings; L. G. Barnes, C. Biermann, R. DeSalle, D. Futuyma, P. Gingerich, J. Powell, R. Sokal and C. Sturmbauer for discussion; and E. Prager for suggesting the myoglobin analysis. M.C.M. is Aspirant at the Fonds National de la Recherche Scientifique de Belgique; G.O. and A.M. are supported by grants from the NSF.

Colour is what the eye sees best

A. Chaparro*, C. F. Stromeyer III*†, E. P. Huang*, R. E. Kronauer* & Rhea T. Eskew Jr‡

* Division of Applied Sciences and † Department of Psychology, Harvard University, Cambridge, Massachusetts 02138, USA
‡ Department of Psychology, Nightingale Hall, Northeastern University, Boston, Massachusetts 02115, USA

IT has been argued by Watson, Barlow and Robson[1] that the visual stimulus that humans detect best specifies the spatial–temporal structure of the receptive field of the most sensitive visual neurons. To investigate 'what the eye sees best' they used stimuli that varied in luminance alone. Because the most abundant primate retinal ganglion cells, the P cells, are colour-opponent[2–4], we might expect that a coloured pattern would also be detected well. We generalized Watson *et al.*'s study[1] to include variations in colour as well as luminance. We report here that our best detected coloured stimulus was seen 5–9-fold better than our best luminance spot and 3–8-fold better than Watson's best luminance stimulus. The high sensitivity to colour is consistent with the prevalence and high colour contrast-gain of retinal P cells, and may compensate for the low chromatic contrasts typically found in natural scenes.

Observers (indicated by their initials) fixated the centre of a bright, uniform yellow field (Fig. 1*a*) which was briefly modulated in luminance or colour. The small test spot fell on the central fovea where there are only long-wave (L) and middle-wave (M) cones[5]. The field was composed of red, green and yellow monochromatic lights[6]. By adjusting the amplitude ratio of incremental and decremental red and green components in the flash, the flash could be made to stimulate the L and M cones in any desired ratio, positive or negative.

To compare sensitivity for luminance and chromatic stimuli one must express the intensities of the stimuli in commensurate units. We did this by calculating the effect of the test flash on the L and M cones, expressed as relative modulation or contrast, $\Delta L/L$ and $\Delta M/M$, in which the numerator represents the change in cone quantal catch produced by the test, and the denominator represents the cone quantal catch produced by the background. Each flash is represented as a vector in the cone contrast coordinates of Fig. 1*b*. Flashes on the horizontal axis stimulate L cones alone (the M cones are silenced), whereas flashes on the vertical axis stimulate M cones alone. Figure 1*b* depicts luminance and

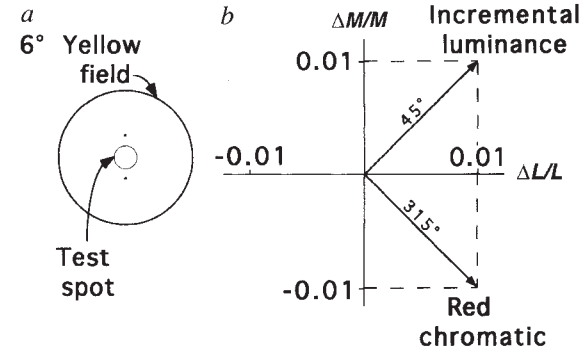

FIG. 1 *a*, The small test flash is presented in the centre of a bright, uniform yellow field (~3,000 trolands, metameric with 580 nm). Fixation is guided by the two black points. Stimuli were seen in a monocular maxwellian view, designed largely to correct for the eye's chromatic aberrations[6]. *b*, Luminance and red chromatic test vectors of equivalent magnitude in the cone contrast coordinates, $\Delta M/M$, $\Delta L/L$. The luminance and chromatic flashes produce equal contrasts in the L and M cones, with the M cone contrast inverted for the chromatic flash. Luminance increments and decrements have vector angles of 45 and 225°; green and red chromatic tests have angles of 135 and 315°. The luminance flash conventionally has contrast $c = \Delta$ luminance/mean luminance, and $c = \Delta L/L = \Delta M/M$.

TABLE 1 Parameters of best detected luminance and chromatic stimuli

		Spot size	Duration	Contrast	Contrast energy, log deg^2 s
A.C.	LUM	10′	55 ms	0.029	−6.00
	CHR	10′	140 ms	0.0063	−6·92
C.F.S.	LUM	5′	55 ms	0.067	−5.87
	CHR	15′	140 ms	0.0066	−6.52
R.T.E.	LUM	5′	55 ms	0.082	−5.69
	CHR	15′	100 ms	0.0076	−6.55
Ref. 1	LUM	18′	50 ms	0.0236	−5.60

Comparison of spatial and temporal parameters of the optimally detected luminance (LUM) and chromatic (CHR) flashes. Thresholds are specified as both contrast and contrast energy.

red chromatic stimuli of equivalent contrast. A simple sign inversion of the M cone contrast distinguishes the two test flashes. The luminance flash increases L and M contrast equally and appears as a bright yellow flash; the red chromatic flash increases L contrast and decreases M contrast equally and appears as a red shift equiluminant with the background. Thresholds were measured for the full range of test vectors, using a temporal two-interval forced-choice method that estimates the 82% detection level[7].

The threshold contour is expected to reveal two linear detection mechanisms (Fig. 2*a*), a red-green chromatic mechanism and a luminance mechanism. The red-green mechanism responds equally and oppositely to L and M contrast, producing a slope of +1.0 (solid lines). Such a mechanism is revealed by psychophysics[8–10] and by measurements of macaque red-green P (ref. 11) and lateral geniculate nucleus cells[12]. The luminance mechanism sums the L and M contrasts of the same sign[13], and thus the threshold contour has a negative slope (dashed lines) indicating the equiluminant direction, a slope not necessarily of −1.0.

Figure 2*b* shows thresholds for flashes of 5 and 10 minutes of arc diameter and 200 ms duration. The ratio of chromatic:luminance sensitivity (solid versus dotted arrows) is 3.1 for the 5′ spot and 4.0 for the 10′ spot. Contours for the other observers have red-green slopes of 1.0 and similar aspect ratios. Red and green chromatic flashes could be distinguished as accurately as the flashes were detected, further indicating that a chromatic mechanism mediates detection.

We next searched for the size and duration for optimal detection of the luminance and chromatic spots. According to Watson *et al.*[1], the best-detected stimulus has the lowest contrast energy, E,

$$E = \int\int\int c^2(x, y, t)\, dx\, dy\, dt$$

where the square of the contrast, c, is integrated over the spatial and temporal dimension of the test (x, y, t). This stimulus identifies the spatial-temporal receptive field of the most sensitive detector[1,14,15]. For a luminance stimulus $c = \Delta L/L = \Delta M/M$. For the more general case where $\Delta L/L \neq \Delta M/M$, the contrast energy can be specified as

$$E = \frac{1}{2}\int\int\int\left\{\left(\frac{\Delta L}{L}(x, y, t)\right)^2 + \left(\frac{\Delta M}{M}(x, y, t)\right)^2\right\} dx\, dy\, dt.$$

Figure 3*a* and *b* shows contrast energy thresholds for luminance and chromatic spots of 5, 10 and 15′ as a function of duration. The lowest luminance and chromatic thresholds occur at 55 ms and 140 ms, respectively. Figure 3*c* shows thresholds as a function of size, with duration roughly optimal. The luminance spots have broad minima at 5 to 15′, consistent with Watson *et al.*, whereas the chromatic minima are nearer 15′. Thus the chromatic pathways have greater spatial[16,17] and temporal summation[18,19], providing further evidence for different signal processing streams. Note that chromatic sensitivity is higher than luminance sensitivity even for stimuli matched to the optimal luminance spots (for example 10′, 60 ms; Fig. 3*a*, *b*). Table 1 lists the optimal luminance and chromatic spots for three observers, along with the data of Watson *et al.* Results for the luminance spots are quite consistent for all observers. The contrast energy thresholds of the chromatic spots are 5–9-fold lower than the luminance spots, and 3–8-fold lower than the optimal drifting luminance grating of Watson *et al.* We have examined only spots; lower thresholds might be obtained with other chromatic patterns that better match the receptive fields of chromatic neurons.

We now show that the signal:noise ratio of an ensemble of retinal P cells is compatible with the high chromatic sensitivity. P cells have overlapping opponent L-centres and M-surrounds (or vice versa) of comparable weights[11,20]. The independent signals from many P cells may add within a detector. In detecting a red flash, for example, the detector may add signals from P cells with L-on and M-off centres, and the density of these cells in the fovea is similar to the cone density[21]. Thus if the retinal area per cone is α, N is the number of P cells covering an area $A = N\alpha$. The impulses summed from these cells over T seconds is $NTc\gamma$, where c is stimulus contrast and γ is a cell's contrast gain. The spontaneous impulse count is $NT\rho$, where ρ is the spontaneous rate of a single cell, and the corresponding variance is $\sim 0.7NT\rho$ (R. M. Shapley, personal communication). When the stimulus matches the ideal detector[15] in A and T, the 82% detection level ($d' = 1.29$) is achieved at a contrast $\hat{c} = (1.29)(0.7NT\rho)^{1/2}/NT\gamma$ (from the relation $d' = \text{signal}/\sigma_n$). The corresponding value of E_{min} for the detector is given by

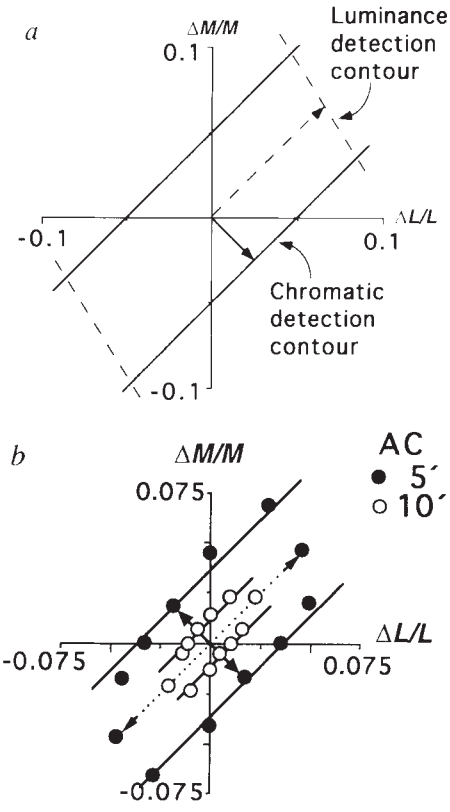

FIG. 2 *a*, Hypothetical threshold contours for luminance and red-green chromatic mechanisms that respond to, respectively, a linearly weighted sum and difference of the L and M cone contrasts. The dashed arrow represents a threshold-level luminance flash; the solid arrow, a threshold-level red chromatic flash. *b*, Threshold contours for 200 ms flashes of 5 and 10′ diameter. The contours are elongated along the luminance axis, revealing greater chromatic sensitivity. The lines drawn near the data have a slope of 1.0.

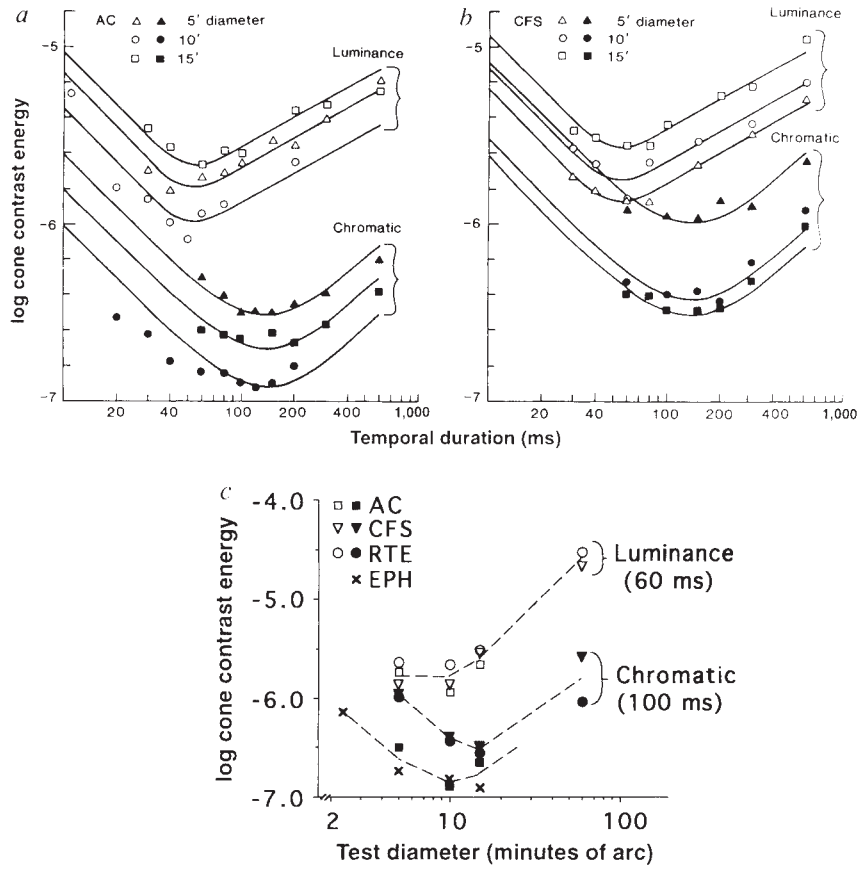

FIG. 3 *a, b*, Contrast energy thresholds (log deg^2 s) for test flashes of 5, 10 and 15′ diameter as a function of duration. The minima estimate the optimal duration for the luminance and chromatic flashes. The fitted curves, derived from mean luminance and mean chromatic data, are of the form $y \propto (x^{-a} + x^b)^{1/a}$, with an asymptotic descending slope, $-a/a = -1.0$ (Bloch's law for temporal integration) and an asymptotic ascending slope of b/a (0.56 for chromatic and 1.0 for luminance). *c*, Contrast energy thresholds as a function of flash diameter, with duration near optimal. Observer E.P.H.'s 200-ms, chromatic flashes were added for comparison.

$\hat{c}^2 AT = (1.29)^2 0.7\rho\alpha/\gamma^2$, which is independent of both N and T. Plausible values are $\alpha = 7 \times 10^{-5}$ deg^2 for the area per cone[22], $\rho = 25$ impulses per s for a cell's spontaneous rate[23,24] and $\gamma = 4$ impulses per s per % contrast for a cell's contrast gain for chromatic patterns (ref. 25; R. M. Shapley, personal communication). The resulting E_{min} of -7.9 log deg^2 s is a log unit below our lowest chromatic energy thresholds. For a luminance stimulus, the P cell contrast gain is only $\gamma = 0.8$ impulses per s per % contrast[26], and the corresponding E_{min} is -6.5 log deg^2 s, about 0.6 log unit below our best luminance energy thresholds. This estimated sensitivity is probably too high because many P cells have low spatial frequency luminance attenuation[27] and thus would not respond optimally to the central regions of the test spot. We have not attempted similar calculations for the M cells, for it is not clear how well they are represented in the central fovea[27,28]. The high sensitivity to colour can thus be explained by properties of the P cells, their prevalence, high chromatic gain and noise characteristics, provided that the signals are effectively summated. □

Received 22 May; accepted 16 November 1992.

1. Watson, A. B., Barlow, H. B. & Robson, J. G. *Nature* **302,** 419–422 (1983).
2. Gouras, P. *J. Physiol., Lond.* **199,** 533–547 (1968).
3. Perry, V. H. & Cowey, A. *Vision Res.* **25,** 1795–1810 (1985).
4. Perry, V. H., Oehler, R. & Cowey, A. *Neuroscience* **12,** 1101–1123 (1984).
5. Williams, D. R., MacLeod, D. I. A. & Hayhoe, M. H. *Vision Res.* **21,** 1341–1356 (1981).
6. Cole, G. R., Stromeyer, C. F. III & Kronauer, R. E. *J. opt. Soc. Am.* A**7,** 128–140 (1990).
7. Watson, A. B. & Pelli, D. G. *Percept. Psychophys.* **33,** 113–120 (1983).
8. Noorlander, C., Heuts, M. J. G. & Koenderink, J. *J. opt. Soc. Am.* **71,** 453–459 (1981).
9. Stromeyer, C. F. III, Cole, G. R. & Kronauer, R. E. *Vision Res.* **25,** 219–237 (1985).
10. Thornton, J. E. & Pugh, E. N. Jr *Science* **219,** 191–193 (1983).
11. Lee, B. B., Martin, P. R. & Valberg, A. *J. Physiol., Lond.* **414,** 223–243 (1989).
12. Derrington, A. M., Krauskopf, J. & Lennie, P. *J. Physiol., Lond.* **357,** 241–265 (1984).
13. Stromeyer, C. F. III, Cole, G. R. & Kronauer, R. E. *Vision Res.* **37,** 1113–1137 (1987).
14. van Trees, H. L. *Detection, Estimation, and Modulation Theory* (Wiley, New York, 1968).
15. Pelli, D. G. in *Vision: Coding and Efficiency* (ed Blakemore, C.) (Cambridge Univ. Press, Cambridge, 1990).
16. Mullen, K. *J. Physiol., Lond.* **359,** 381–400 (1985).
17. King-Smith, P. E. & Carden, D. *J. opt. Soc. Am.* **66,** 709–717 (1976).
18. Kelly, D. H. & van Norren, D. *J. opt. Soc. Am.* **67,** 1081–1091 (1977).
19. Smith, V. C., Bowen, R. W. & Pokorny, J. *Vision Res.* **24,** 653–660 (1984).
20. Reid, R. C. & Shapley, R. M. *Nature* **356,** 716–718 (1992).
21. Schein, S. J. *J. comp. Neurol.* **269,** 479–505 (1988).
22. Hirsch, J. & Curcio, C. C. *Vision Res.* **29,** 1095–1101 (1989).
23. Troy, J. B. & Lee, B. B. *Invest. Ophthalmol. Vis. Sci.* **32** (suppl.), 905 (1991).
24. Crook, J. M., Lange-Malecki, B., Lee, B. B. & Valberg, A. *J. Physiol., Lond.* **396,** 205–224 (1988).
25. Shapley, R. M., Reid, R. C. & Kaplan, E. *Invest. Ophthalmol. Vis. Sci.* **32** (suppl.), 115 (1991).
26. Purpura, K., Kaplan, E. & Shapley, R. M. *Proc. natn. Acad. Sci. USA* **85,** 4534–4537 (1988).
27. Derrington, A. M. & Lennie, P. *J. Physiol.*, Lond. **357,** 219–240 (1984).
28. Kaplan, E., Lee, B. B. & Shapley, R. M. in *Progress in Retinal Research* Vol. 9 (eds Osborne, N. & Chader, J.) (Pergamon, Oxford, 1990).

ACKNOWLEDGEMENTS. We thank D. Pelli and R. M. Shapley for their comments. Research was supported by the NIH, USAF Office of Scientific Research and the Ford Foundation.

Innervation directs receptor synthesis and localization in *Drosophila* embryo synaptogenesis

Kendal Broadie & Michael Bate

Department of Zoology, University of Cambridge, Downing Street, Cambridge CB2 3EJ, UK

IN the *Drosophila* embryo, motor neurons form stereotyped synapses (neuromuscular junctions) on identified muscles[1–3]. We have used a mutant (*prospero*) that removes or delays innervation[4,5] to assay the role of the presynaptic motor neuron in the development of the receptive field of the postsynaptic muscle. *prospero* (*pros*) is not expressed in the muscles or their precursors. Here we find that the muscle defines the correct synaptic zone in the absence of the motor neuron by restricting putative guidance molecules to this specialized membrane region. Furthermore, the muscle expresses functional transmitter receptors at the correct developmental time without innervation. On the other hand, the muscle